

# Effect of Freestream Conditions on the Far Wake of a Circular Cylinder

John M. Cimbala\* and Mark V. Krein†

*Pennsylvania State University, University Park, Pennsylvania 16802*

**Hot-wire anemometry was incorporated to measure the frequency spectra at various downstream locations in the wake of a two-dimensional circular cylinder at a Reynolds number of  $1.4 \times 10^5$ . Two different freestream conditions were imposed on the wake to study the dependence of the wake spectra on background noise. The prominent frequencies observed in the wake showed significant dependence on freestream conditions. Moreover, all of the spectral peaks could be identified as sums or differences between the Karman frequency and prominent freestream frequencies or their harmonics or sums or differences between two or more prominent freestream peaks independent of Karman frequency. This implies that the far-wake structures arise due to hydrodynamic instability of the wake and that the associated frequencies of these structures are dependent on nonlinear interactions between the existing wake structures and disturbances in the freestream.**

## I. Introduction

It has been shown<sup>1-3</sup> that the Karman vortex street behind a circular cylinder does not continue indefinitely downstream. Instead, by about a hundred or more cylinder diameters, larger-scale vortical structures are observed. There have been two principal views concerning the mechanism leading to the formation of these structures. The first view explains that the larger structures are the result of vortex amalgamation. In other words, the structure observed in the far wake is the direct result of the Karman vortices combining into larger vortex structures.<sup>2,4</sup> The far-wake structures, according to this view, should be highly dependent on the shed vortices and in particular should depend on mutual interaction and distortion of these vortices.<sup>4,5</sup>

The second view attributes the growth of far-wake structures to hydrodynamic instability of the mean-wake profile. This view infers that the downstream structure should eventually be independent of the vortices shed by the body. For example, Cimbala et al.<sup>3</sup> found that the Karman vortex street has largely decayed by the time secondary structures become significant.

The purpose of this research is to shed further light on the mechanism responsible for the growth of structure in the far wake of a bluff body. This entailed the use of a low-turbulence wind tunnel and hot-wire anemometry applied to the wake of a circular cylinder at  $Re_d = 1.4 \times 10^5$ . A two-sensor hot-wire probe was used to measure both streamwise ( $u'$ ) and normal ( $v'$ ) velocity fluctuations. By opening or closing bypass vents in the wind tunnel while maintaining the same mean freestream velocity, two different freestream conditions were imposed on the wake. The two fan operating conditions enabled comparisons to be made between background noise and dominant far-wake frequencies. If the instability view is correct, the far-wake structures should show significant dependence on the background noise. If the amalgamation view is correct, less dependence would be expected.

## II. Facility and Instrumentation

The open-loop wind tunnel used in this investigation had a Plexiglas test section 0.97 by 0.3 m in cross section with a

length of 2.44 m. The tunnel was equipped with a set of bypass vents just downstream of the test section. When open, air was drawn in from the room, which caused a decrease of velocity in the test section. A given freestream velocity could then be obtained by two ways—vents closed with a low-fan speed or vents open with a high-fan speed. For the particular operating condition of  $U_\infty = 1.4$  m/s used exclusively in this experiment, two freestream turbulence intensities,  $u'_{rms}/U_\infty$ , were measured. The first, corresponding to the operating condition with the bypass vents closed, was approximately 0.4%. The second, corresponding to the vent open condition, was about 0.5%.

The circular cylinder used in the experiment was made of a 1.61-mm drill rod and was stretched across the 0.97-m span of the wind tunnel. Two small elliptic sheet-metal plates, machined to a sharp edge, were mounted on either end to minimize end effects. With the plate approximately 40 mm from either wall, the effective aspect ratio of the cylinder was approximately 550. For all cases the freestream velocity  $U_\infty$  was fixed at 1.4 m/s, and the Reynolds number  $Re_d$  was  $1.4 \times 10^5$ .

A two-channel hot-wire anemometer was used in conjunction with low-pass filters to obtain an output signal from single and double sensor hot-wire probes. The single wire probe enabled the measurement of mean velocity profiles, and the dual sensor probe enabled the determination of  $u'$  and  $v'$  fluctuating velocities.

Computer control for data acquisition and hot-wire positioning was accomplished with an AT&T Model 6300 personal computer, a Metrabyte Model DAS-16F high-speed analog to digital interface, and a Metrabyte Model PI012 digital parallel interface.

For data reduction, spectral analysis, and plotting, a VAX 11/780 computer was used in addition to the personal computer. Further details concerning the facility and instrumentation can be found in Ref. 6.

## III. Results

With the cylinder model removed from the wind tunnel, freestream spectra were measured. These are shown in Figs. 1 and 2. As can be seen, there was a marked difference between the vent-open and vent-closed conditions. With the vents open, there was a prominent peak in the spectrum at 102 Hz along with its harmonic at 204 Hz. These are labeled  $f_1$  and  $2f_1$ , respectively, on Fig. 1. Other peaks are labeled and identified (in order of decreasing magnitude) as follows:  $f_2 = 9$  Hz,  $f_3 = 76$  Hz,  $f_4 = 111$  Hz,  $f_5 = 180$  Hz,  $f_6 = 58$  Hz, and  $f_7 = 69$  Hz. With the vents closed (Fig. 2), the freestream contained peaks of  $f_1 = 43$  Hz,  $2f_1 = 86$  Hz,  $f_2 = 180$  Hz, and  $f_3 = 171$  Hz.

Received Oct. 25, 1988; revision received Aug. 21, 1989. Copyright © 1989 by the American Institute of Aeronautics and Astronautics, Inc. All rights reserved.

\*Associate Professor, Department of Mechanical Engineering, Member AIAA.

†Graduate Research Assistant, Department of Mechanical Engineering; currently with Sverdrup Technology, Inc., Cleveland, OH.

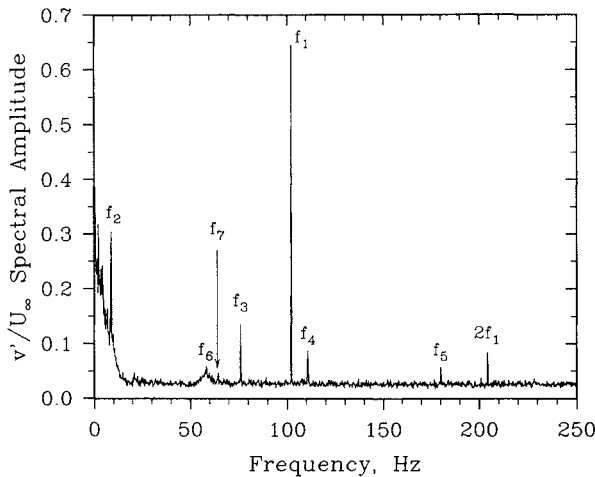


Fig. 1 The  $v'/U_\infty$  freestream frequency spectrum,  $U_\infty = 1.4$  m/s, vents open.

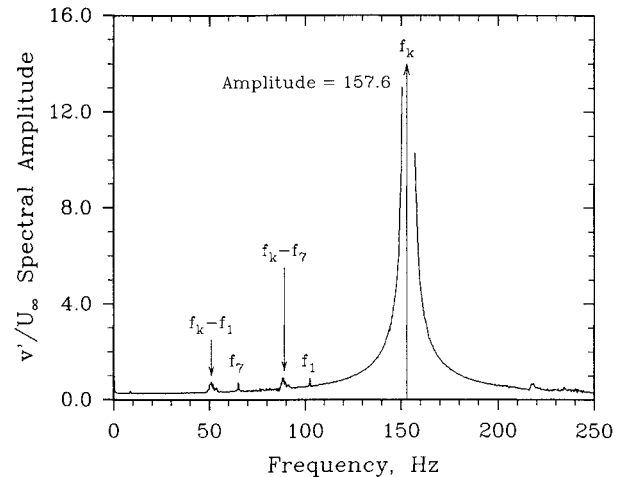


Fig. 3 The  $v'/U_\infty$  freestream frequency spectrum at  $x/d=25$ ,  $Re_d = 1.4 \times 10$ , vents open.

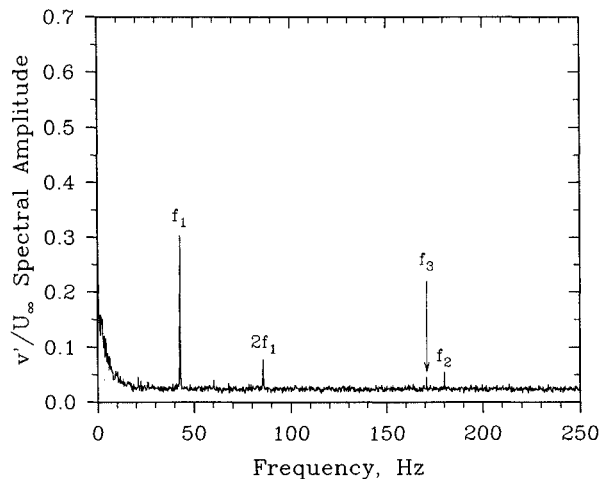


Fig. 2 The  $v'/U_\infty$  freestream frequency spectrum,  $U_\infty = 1.4$  m/s, vents closed.

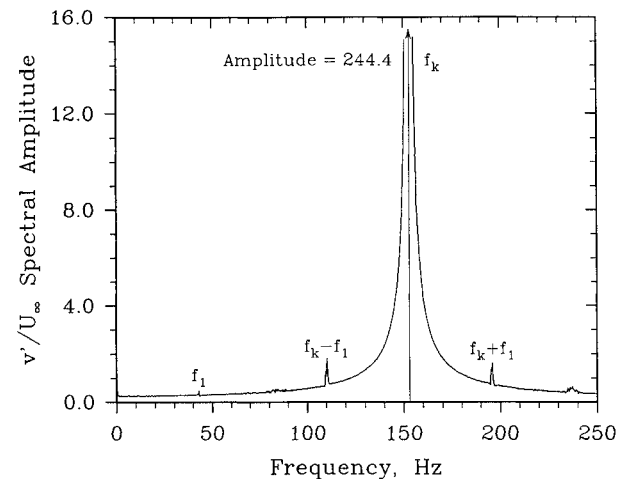


Fig. 4 The  $v'/U_\infty$  freestream frequency spectrum at  $x/d=25$ ,  $Re_d = 1.4 \times 10$ , vents closed.

Comparing these, the only significant common frequency is 180 Hz. The other peaks are apparently related to the fan speed or noise from the vents since everything else was kept constant. The disturbances are most likely acoustic in nature. In all spectra shown, the frequency resolution is 0.244 Hz.

With the cylinder installed, wake spectra were then measured for both freestream conditions at several  $x$  locations. In all of the results presented below, the  $y$  location was chosen as that where the turbulence level was maximum. This was typically at or near an inflection point of the mean-velocity profile.

At downstream location  $x/d=25$ , the Karman shedding frequency can easily be identified. Spectra are shown in Figs. 3 and 4 for the vents-open and vents-closed cases, respectively. In both cases, Karman frequency  $f_k$  is about 153 Hz, and its amplitude is quite large (off the scale in Figs. 3 and 4). Other peaks, orders of magnitude smaller amplitude than  $f_k$ , are also identifiable on these spectra. For the vents-open case,  $f_1$  and  $f_7$ , two of the freestream peaks as well as two additional somewhat broader peaks at 51 and 88 Hz are present. These can be identified as  $f_k - f_1$  and  $f_k - f_7$ , respectively. For the vents-closed case (see Fig. 4), a similar situation is observed. Freestream frequency  $f_1$  as well as  $f_k - f_1$  (110 Hz) and  $f_k + f_1$  (196 Hz) are present.

At  $x/d=50$ , the Karman frequency continues to be the dominant peak for both cases, although its magnitude is substantially decreased. For the vents-open case (Fig. 5), the

same low-frequency peaks observe at  $x/d=25$  are present but have increased somewhat in magnitude. A similar situation occurs for the vents-closed case (see Fig. 6), although additional peaks corresponding to  $2f_1$  and  $f_k - 2f_1$  also appear.

At the downstream location of  $x/d=100$ , the peak at the Karman frequency has decayed to the point where it is no longer the dominant wake frequency. For the vents-open condition (Fig. 7), the peaks observed at  $x/d=50$  (i.e.,  $f_1$ ,  $f_7$ ,  $f_k - f_1$ , and  $f_k - f_7$ ) have grown significantly. A couple of other peaks have also arisen, namely a peak at  $f_3 = 76$  Hz (which is close to the subharmonic of  $f_k$ ) and a peak at 38 Hz, which can be identified as  $f_1 - f_7$ .

For the vents-closed case at  $x/d=100$  (see Fig. 8), the magnitude of the Karman frequency peak has dropped below that of the peak at  $f_k - f_1$ , which is now dominant. In addition, the smaller peaks at  $f_1$ ,  $2f_1$ , and  $f_k - 2f_1$  have grown significantly from their magnitudes observed at  $x/d=50$ . Finally, the small peak at  $f_k + f_1$ , which was observed at  $x/d=50$ , is no longer significant.

At  $x/d=200$ , the Karman frequency  $f_k$  is no longer significant. The dominant peak for the vents-open case (see Fig. 9) occurs at  $f_7$ , whereas the higher-frequency peak at  $f_1$  has decayed somewhat from its magnitude at  $x/d=100$ . The first harmonic of  $f_7$  is also present. Meanwhile, the other peaks, which were observed at  $x/d=100$  (i.e.,  $f_k - f_1$ ,  $f_k - f_7$ ,  $f_1 - f_7$ , and  $f_3$ ) have all increased in amplitude at  $x/d=200$ . In addition two peaks at much lower frequencies, 15 and 23 Hz, have

arisen. The 15 Hz peak can be identified as either  $f_7 - (f_k - f_1)$  or  $(f_k - f_1) - (f_1 - f_7)$ , and the 23 Hz peak can be identified as  $(f_k - f_7) - f_7$ . Finally, some new combinations of the peaks appear at higher frequencies, such as at  $(f_k - f_1) + f_7$  and  $f_3 + f_7$ . It is interesting to point out that most of the peaks in Fig. 9 can alternately be identified as nearly integral multiples of 12.8 Hz.

At  $x/d=200$  with the vents closed (see Fig. 10), the spectrum is not as rich as that with the vents open. The peak at  $f_k - f_1$ , which was dominant at  $x/d=100$ , has decayed. The lower frequency peaks at  $f_1$ ,  $2f_1$ , and  $f_k - 2f_1$ , have grown in magnitude in its stead. Also, a low-frequency peak at 21 Hz has arisen and can be identified as  $(f_k - 2f_1) - f_1$ , which in this case also turns out to be approximately the subharmonic of  $f_1$ . Alternately all of the major peaks labeled in Fig. 10 can be identified as nearly integral multiples of 21 Hz.

At the much further downstream position of 400 diameters, the prominent frequency peaks have again shifted to the left. For the vents-open case (see Fig. 11), the peak at  $f_7$  remains dominant but lower in amplitude, and the higher-frequency peaks have also decayed when compared with the spectrum at  $x/d=200$ . Peaks at frequencies lower than 40 Hz, however, have increased in magnitude. Most of the peaks occur at the same frequencies as observed at  $x/d=200$ , and additional peaks appear, which can all be identified as combinations of previously existing peaks as labeled in Fig. 11.

For the vents-closed case at  $x/d=400$  (see Fig. 12), the peak at  $f_k - 2f_1$  is dominant, and the low-frequency peak at

$(f_k - 2f_1) - f_1$  has amplified considerably. The remaining peaks which were observed at  $x/d=200$  have decayed somewhat. Again this spectrum with the vents closed is not as filled as that with the vents open. This implies that the total area under the spectrum, which is related to the magnitude of  $v'_{rms}$ , is much smaller for the vents-closed condition.

#### IV. Discussion

In the present experiment, the cylinder was identical to the one used by Cimbalá et al.,<sup>3</sup> and measurements were taken at  $Re_d = 1.4 \times 10$  as well. However, the present investigation was conducted in a different wind tunnel facility with two background noise conditions as just described. Careful study of the amplitude spectra at several downstream positions has yielded the following observations.

1) The observed spectra in the wake show extreme sensitivity to freestream conditions present in the wind tunnel.

2) Every peak in the spectra from  $25 \leq x/d \leq 400$  can be identified as a sum or difference of Karman frequency  $f_k$  and a freestream peak or its harmonic or a sum or difference of two freestream peaks. By  $x/d=400$ , however, the number of peaks becomes so large (particularly for the vents-open case) that the spectrum begins to appear chaotic.

3) Most of the spectral peaks can be identified as nearly integral multiples of some low frequency. Some tables illustrating this can be found in Ref. 6.

4) As downstream distance is increased, the associated spectra shift to the left (i.e., toward lower frequency). The magni-

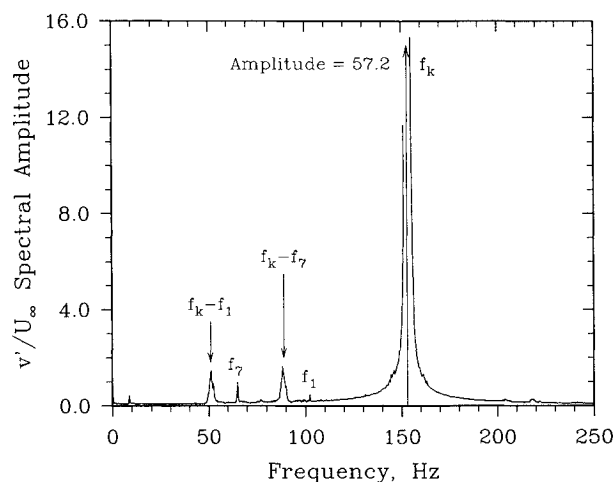


Fig. 5 The  $v'/U_\infty$  freestream frequency spectrum at  $x/d=50$ ,  $Re_d = 1.4 \times 10$ , vents open.

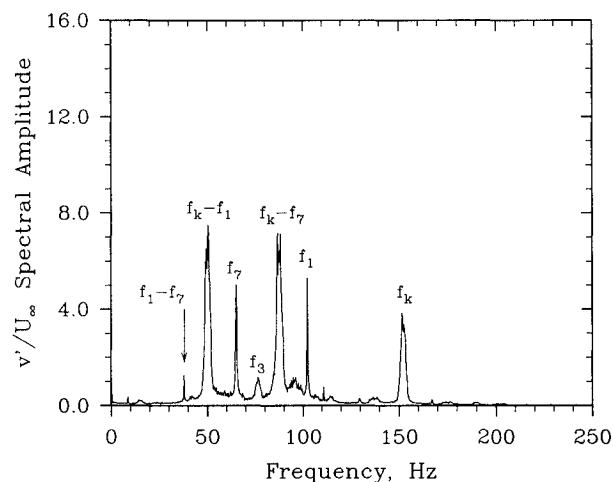


Fig. 7 The  $v'/U_\infty$  freestream frequency spectrum at  $x/d=100$ ,  $Re_d = 1.4 \times 10$ , vents open.

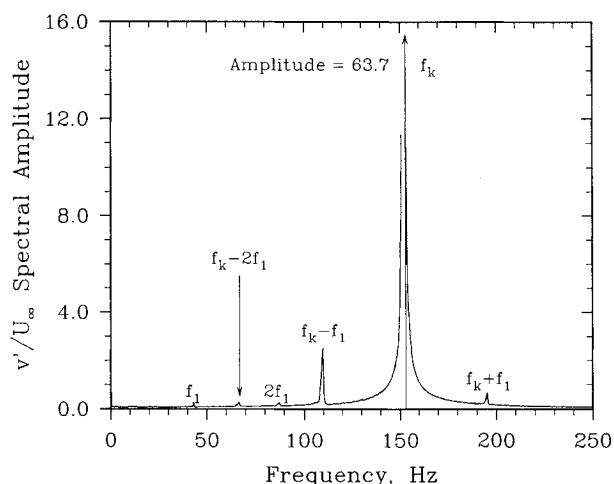


Fig. 6 The  $v'/U_\infty$  freestream frequency spectrum at  $x/d=50$ ,  $Re_d = 1.4 \times 10$ , vents closed.

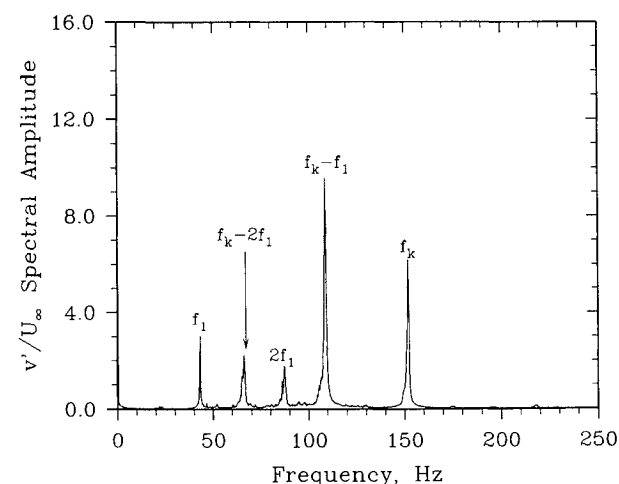


Fig. 8 The  $v'/U_\infty$  freestream frequency spectrum at  $x/d=100$ ,  $Re_d = 1.4 \times 10$ , vents closed.

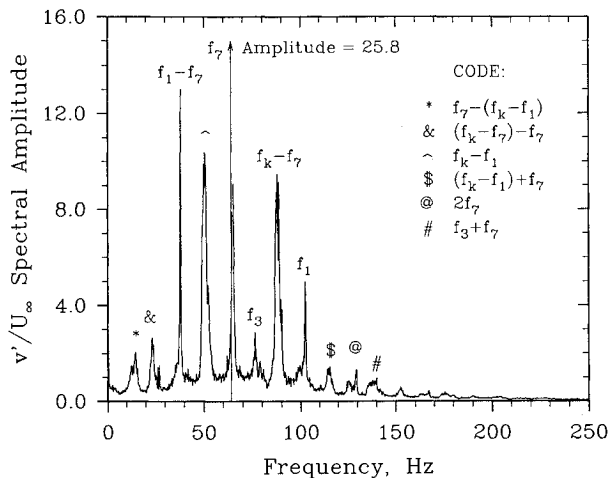


Fig. 9 The  $v'/U_\infty$  freestream frequency spectrum at  $x/d=200$ ,  $Re_d = 1.4 \times 10$ , vents open.

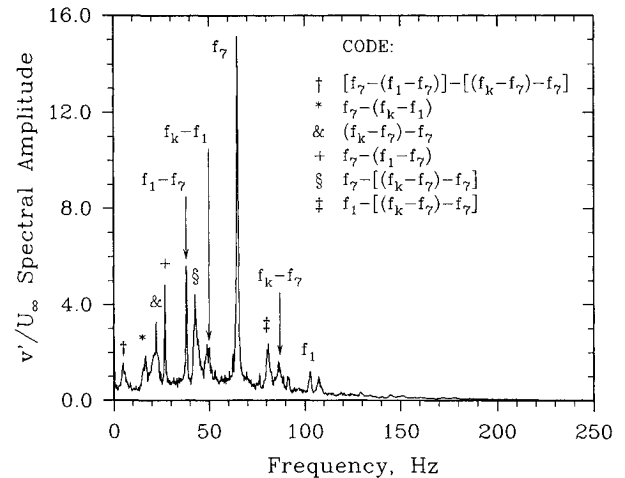


Fig. 11 The  $v'/U_\infty$  freestream frequency spectrum at  $x/d=400$ ,  $Re_d = 1.4 \times 10$ , vents open.

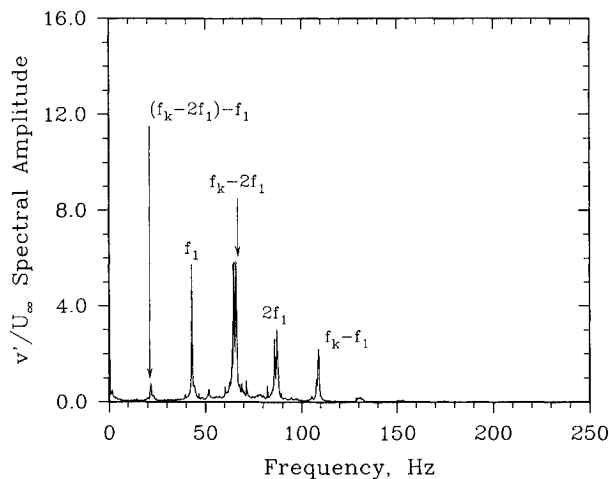


Fig. 10 The  $v'/U_\infty$  freestream frequency spectrum at  $x/d=200$ ,  $Re_d = 1.4 \times 10$ , vents closed.

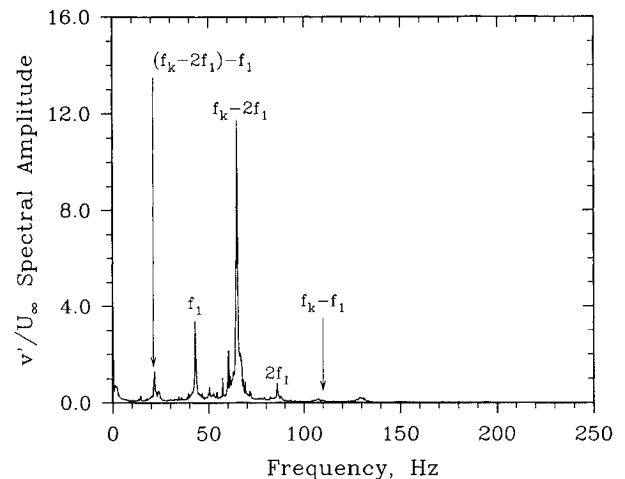


Fig. 12 The  $v'/U_\infty$  freestream frequency spectrum at  $x/d=400$ ,  $Re_d = 1.4 \times 10$ , vents closed.

tude of any particular frequency first rises then decays with increasing  $x$ . A good example is the peak at  $f_1 = 102$  Hz for the vents-open case. Its spectral magnitude in the freestream (with no cylinder in the wind tunnel) is about 0.65. This magnitude grows to about 5.5 at  $x/d = 100$ , drops to about 5 at  $x/d = 200$ , and then drops to about 1 at  $x/d = 400$ .

Let us now examine some possible interpretations of these observations. As discussed in the Introduction, there are two principal views concerning the growth of large-scale structures in the far wake. The first attributes the growth to mutual interaction, distortion, and amalgamation of the Karman vortices. Meiburg<sup>4</sup> argues for this interpretation based on numerical stability calculations. By specifying initial conditions in which an infinite array of vortices is disturbed periodically in space, he was able to observe vortex amalgamation and therefore the rise of lower frequencies in the spectra. Furthermore, his calculations predict that the frequencies which dominate the far-wake spectra are all integral multiples of some low frequency which is specified by his initial disturbance. He supports his interpretation by pointing out that most of the prominent peaks in the experimental spectra of Cimbalá et al.<sup>3</sup> are also nearly integral multiples of some low frequency.

The most significant difference between Meiburg's analysis and the present experimental data is this: The small frequency just referred to must be supplied by the initial conditions in the numerical simulations. (This small frequency represents the imposed periodicity of the whole flowfield.) On the other hand, the present experiments show that in reality, this low frequency does not even exist in the freestream spectra. Fur-

thermore, successive sums and differences of prominent frequencies in the near wake and freestream eventually lead to far-wake spectra in which almost all of the peaks are nearly integral multiples of a small frequency, in spite of the absence of that frequency in the freestream. Finally, Meiburg's analysis is not physically realistic since he assumes an infinite array of Karman vortices, when in reality the Karman vortex street rapidly disappears with downstream distance.<sup>3</sup>

Some very recent stability calculations<sup>7,8</sup> may provide a better explanation for the observed spectral behavior. Sauliere and Huerre,<sup>7</sup> for example, predict nonlinear interactions between sinuous and varicose instability modes in a wake profile. Both of these modes can exist in the wake, but their frequencies will be quite different. Subharmonic interaction between the two modes can lead to a kind of "beating" phenomenon, or "phase jitter," which will manifest itself in the frequency spectrum as a low frequency. Other peaks in the spectrum may be due to further nonlinear interactions between this frequency and the other frequencies. Somewhat similar results have also been obtained recently by Fleming.<sup>8</sup> These stability predictions appear to agree fairly well with the experimental spectra reported here. In particular, the phase jitter caused by nonlinear interaction between the sinuous and varicose modes provides a possible source for the observed low frequencies and their multiples, even though these frequencies do not appear prominent in the freestream spectra.

The most probable mechanism for the growth of large-scale, far-wake structures is that of hydrodynamic instability as argued by Cimbalá et al.<sup>3</sup> As one moves further and further

downstream in a wake, its width increases whereas its centerline velocity defect decreases, both of which lead to changes in the hydrodynamic stability characteristics of the mean-wake profile. Specifically, the range of unstable (amplifying) frequencies shifts further to the left (i.e., toward lower frequencies) as  $x$  increases. While this shift is rather smooth for turbulent wakes and the spectra are quite broad,<sup>3</sup> laminar wakes shift much more abruptly with certain discrete frequencies dominating the spectra.

Cimbala et al.<sup>3</sup> originally suggested that prominent freestream frequencies are selectively chosen to be amplified by the wake according to the instability characteristics of the mean-wake profile. Instead it appears from the present experiments that a frequency representing the difference between  $f_k$  and a prominent freestream frequency is more likely to be amplified than the prominent freestream frequency itself. This is not surprising since Desruelle<sup>9</sup> has shown conclusively that the response frequency in a wake is equal to the absolute value of the difference between the Karman frequency and the excitation frequency when the latter is of long wavelength compared to the former. This argument can be extended to the far wake where the Karman frequency has disappeared entirely. In this case, the response frequency would be expected to be a difference between available frequencies in the wake—either from the wake itself or from the freestream. This is exactly what was found in the present experiments. For example, under open-vent conditions, the most prominent frequencies at  $x/d \approx 100$  were differences like  $f_k - f_1$  or  $f_k - f_7$ , whereas at  $x/d \approx 400$ , the most prominent frequencies were differences like  $f_1 - f_7$ ,  $f_7 - (f_1 - f_7)$ ,  $f_7 - f_k$ , and  $f_7$  itself.

Further more, such nonlinear interactions between available frequencies would be expected to be more common when any prominent frequencies are present in the freestream. This is indeed the case as shown by the present experiments. Namely, under vents-open conditions, the freestream contained seven identifiable frequency peaks and one harmonic, whereas the vents-closed condition produced only three peaks and one harmonic. Consequently, the wake spectra for the vents-open case show significantly more discrete frequencies than do those for the vents-closed case. (Compare, for example, Fig. 9 with Fig. 10, or Fig. 11 with Fig. 12.)

In the vents-open freestream spectrum (see Fig. 1), the peak labeled  $f_7$  is very small compared to the others. Why then does  $f_k - f_7$  emerge as a dominant frequency far downstream when others (such as combinations of  $f_k$  and  $f_2$ ,  $f_4$ ,  $f_5$  or  $f_6$ ) are never amplified? One possibility is vibration of the cylinder. The authors have calculated that 89 Hz is one of the natural vibrational modes of the rod. This happens to be very close to  $f_k - f_7$  (88 Hz). This frequency may have initially amplified in-

stead of the others due to feedback and reinforcement of vibrations of the cylinder.

## V. Conclusions

In summary, freestream noise has been shown to play an important role in the development of vortical structures in the far wake of a circular cylinder at  $Re = 1.4 \times 10$ . All of the spectral peaks in the wake can be identified as arising from nonlinear interactions (i.e., differences or sometimes sums) between prominent freestream peaks and peaks available in the wake itself. These observations support the hypothesis that hydrodynamic instability of the wake is responsible for the growth of far-wake structures.

## Acknowledgments

The authors appreciate the support of the Pennsylvania State University's Department of Mechanical Engineering, which provided the facility and equipment for this research project. In addition, we would like to thank H. Nagib and K. Stuber with whom we had worthwhile discussions concerning the interpretation of our data when it was presented at the First National Fluid Dynamics Congress in Cincinnati, Ohio, during July 1988.

## References

- <sup>1</sup>Taneda, S., "Downstream Development of Wakes Behind Cylinders," *Journal of the Physics Society of Japan*, Vol. 14, No. 6, 1959, pp. 843-848.
- <sup>2</sup>Matsui, T., and Okude, M., "Vortex Pairing in a Karman Vortex Street," *Proceedings from the Seventh Biennial Symposium on Turbulence*, Rolla, MO.
- <sup>3</sup>Cimbala, J. M., Nagib, H. M., and Roshko, A., "Large Structure in the Far Wakes of Two-Dimensional Bluff Bodies," *Journal of Fluid Mechanics*, Vol. 190, 1988, pp. 265-298.
- <sup>4</sup>Meiburg, E., "On the Role of Subharmonic Perturbations in the Far Wake," *Journal of Fluid Mechanics*, Vol. 177, 1987, pp. 83-107.
- <sup>5</sup>Meiburg, E., "Experimental and Numerical Investigation of the Three-Dimensional Transition in Plane Wakes," *Journal of Fluid Mechanics*, Vol. 190, 1985, pp. 190.
- <sup>6</sup>Krein, M. V., "Freestream Effects on the Far Wake of a Two-Dimensional Bluff Body," M.S. Thesis, Dept. of Mechanical Engineering, The Pennsylvania State University, University Park, PA, 1987.
- <sup>7</sup>Sauliere, J., and Huerre, P., "Spatial Chaos and Nonlinear Interactions in Wake-Shear Layers," *Bulletin of the American Physical Society*, Vol. 32, No. 10, 1987, p. 2071.
- <sup>8</sup>Fleming, M. F., "Secondary Instability in the Far Wake," M.S. Thesis, Dept. of Mechanical and Aerospace Engineering, Illinois Institute of Technology, Chicago, IL, 1987.
- <sup>9</sup>Desruelle, D., "Beyond the Karman Vortex Street," M.S. Thesis, Dept. of Mechanical and Aerospace Engineering, Illinois Institute of Technology, Chicago, IL, 1983.